Applications of Geometric Phase in Optics

Enrique J. Galvez
Department of Physics and Astronomy
Colgate University

Abstract

In the last fifteen years several manifestations of geometric phase in optics have been discovered. The most studied manifestations are spin redirection phase and Pancharatnam phase. A new phase on the transformations of optical beam modes has begun to be studied. This article reviews the principles of these phases and discusses the applications that have been proposed and reported in the literature.

I. Introduction

In 1984 Berry reported on the analysis of an aspect of dynamical systems that had been largely ignored before [1]. It involved the phase that a physical system acquires when it travels a path in either parameter space or state space. Consider for instance a beam of light traveling on a certain path in real space. A calculation of the phase of the wave after the path cannot be based only on the optical path length or the time evolution of the Hamiltonian, a phase that is now referred to as the dynamical phase. Berry pointed out that there is an additional phase that one must consider that depends on the geometry of the path. This phase has become known as *Berry's phase*. Much work has been devoted to the study of this phase [2], which has been found to be ubiquitous to dynamical systems [3]. The initial formulation was made for quantum systems, but since then it has been generalized to classical systems, where it is also known as the *Hannay angle* [4]. However, there is a debate on the physical origin of this phase: quantal or classical [5]. In its most general form, this phase is known as the *geometric phase.*

Although manifestations of this phase have been reported in many different settings (see for example Ref. [3]), perhaps it is in optics where it has had the greatest impact. The studies of two manifestations of geometric phase in optics, known as *spin redirection phase* and *Pancharatnam phase*, have reached enough maturity that applications based on them now abound. A new phase involving the transformations of modes of light beams has only begun to be investigated, but potential applications are already visible. The purpose of this article is to present the applications of geometric phase in optics demonstrated or proposed to this date. The following three sections will be devoted to the three known phases. A fourth section concludes with a discussion of combined phases and other potential geometric phases in optics.

II. Spin Redirection Phase

When a light beam travels in a three-dimensional (off-plane) path it acquires a geometric phase that depends on the path traveled by the beam. Suppose that a circularly polarized beam describes a path that coils like a helix (e.g., by traveling inside an optical fiber) and subsequently returns to its original propagation direction. After describing this path, its phase will differ from the one gained by traveling the same distance, but in a straight trajectory. The extra phase comes from the additional winding of the fields of the beam created by the coiled path. Bringing a mechanical analogy, it would be the extra winding of the phase of a spring whose axis is coiled. This is the spin redirection geometric phase, also known as "coiled-light" phase, or the "Rytov-Vladimirskii" phase. The latter name comes from an early anticipation of this phase [6,7]. This effect falls into a category of mechanical systems involving rotating rotators that have been studied within a classical framework but recently revisited through the concept of geometric phase.

A first application of this phase is the phase shifting of circularly polarized light via a coiled optical path. The sign of this phase will depend on the helicity σ of the light spin ($\sigma = +1$ for left circularly polarized light and $\sigma = -1$ for right circularly polarized light), and on the handedness of the coiled path. A linearly polarized beam of light, which can be expressed as a linear superposition circularly polarized states of opposite helicity, will have its plane of polarization rotated via the equal and opposite geometric phases acquired by the component circularly polarized states [8]. Thus the geometric phase can be obtained through topological arguments: it is a manifestation of parallel transport on a curved surface [9]. In this case the curved surface is the unit sphere of directions of the light spin vector. The closed path on the surface of the sphere is formed by mapping the spin vectors of the light to the origin of the sphere and connecting the tip of the vectors. The Gauss-Bonett theorem reduces the phase accumulated via parallel transport to the area Ω enclosed by the path [10]. An example of a coiled optical fiber is shown in Fig. 1a. The tip of the spin vector describes a path on the sphere of directions like the one shown in Fig. 1b. The sign of Ω will be positive for clockwise paths as seen from the center of the sphere, and negative for the opposite sense. Thus, the geometric phase for circularly polarized beams can be expressed as:

$$\Phi_{gp} = -\sigma\,\Omega. \qquad (1)$$

The first demonstration of coiled-light geometric phase came by sending an optical beam through a coiled optical fiber [11]. The experiment involved measuring the rotation of the polarization of a linearly polarized light beam traveling through the fiber. For the right-handed coil of the optical fiber of Fig. 1a the rotation of the linear polarization will be counter-clockwise as seen from the end of the fiber looking into it. This rotation was also anticipated by Ross based on differential geometry [12].

This system can be used as a phase shifter of circular polarization or as a linear (or elliptical) polarization rotator. For elliptical polarization, the rotation of the semi-major axis of the ellipse is coupled to the phase shift. Conversely, one can obtain a measure of the deformation of a wound optical fiber by a measurement of the polarization of the light emerging from the fiber. Indeed coiled fibers of different geometries (i.e., of varying radius or pitch) have been proposed as mechanical transducers [13]. A Sagnac-type of

interferometer using a coiled fiber can be used to introduce purely geometrical phases. This has been done with a cube beam splitter [14] and with a fiber-optic 50-50 splitter [15]. The advantage of the geometric-phase-based system is that the phase depends only on the geometry of the coil, and thus is independent of the fiber material. Coiled paths *within* a few-mode graded-index optical fiber have been measured to yield geometric phases on the polarization of light beams [16,17] and on the phase profile of beams carrying optical vortices [18].

The path on the sphere of directions does not need to be closed. In such a case the phase is obtained by closing the path on the sphere of directions with a geodesic [19,20]. The geometric paths do not need to be continuous either. This encompasses discrete directions obtained by reflections using mirrors [21]. In such a case one considers the path on the sphere of spin directions, taking into consideration the spin reversal after each reflection [22]. The spin after the n-th reflection is therefore defined as

$$\mathbf{k}' = (-1)^n \mathbf{k}, \tag{2}$$

where $\mathbf{k}$ is the unit propagation vector (i.e., taking $2\pi/\lambda = 1$). The path on the sphere of spin directions, or $\mathbf{k}'$-sphere, is composed of points representing the discrete spin directions connected by geodesics. For example, Fig. 2a shows the path of a beam going through four discrete reflections. The initial spin and the spins after each reflection are represented on the $\mathbf{k}'$-sphere of Fig. 2b. The geometric phase is the area enclosed by the curve formed by those points connected by geodesics: $\Phi_{gp} = 2\phi$. In this example the mirrors are assumed to be ideal. Real metallic mirrors behave ideally in the far infrared, and thus can be used to make polarization rotators for far-infrared beams such as CO_2 laser beams [23].

In the visible, ordinary reflectors cannot be used for geometric-phase polarization rotators because the reflectors introduce unequal phases on the *s* and *p* components of the polarization, leaving the light in an undesired polarization state. A solution to this problem is to use coated reflectors designed to preserve the polarization. Shown in Fig. 3a is a recently proposed variation of the Porro image-inverting system, the "variable-angle Porro," where the second prism is allowed to rotate by an angle θ relative to the first prism [24]. With coated right-angle prisms, this system can be used as a variable polarization rotator [25]. Figure 3b shows the path *S* described by the propagation vector $\mathbf{k}$ of the light as it passes through the variable-angle Porro. If helicity preserving mirrors are used then $\mathbf{k}' = \mathbf{k}$ throughout the path. If helicity reversing (ideal) mirrors are used then the light spin $\mathbf{k}'$ describes the curve *C* upon passage through the device. Both curves *S* and *C* enclose the same area and thus have the same accumulated geometric phase $\Phi_{gp} = 2\theta$. Since all of the angles of incidence are fixed to $\pi/4$, a straight forward coating design is sufficient. However, its operation is narrow-band due to the nature of the interference coatings.

Another variable polarization rotator system that follows the variable-angle Porro design uses retro-reflectors that have four orthogonal reflections [25]. The system of reflections, named the "compensating phase-shift" (CPS) system, removes the reflection phase problem. Following Fig. 4, the *x* component (*y* component) of the polarization of the light relative to the first retro-reflector experiences *s*-polarized (*p*-polarized) reflections at the

1st and 4th reflectors and *p*-polarized (*s*-polarized) reflections at the 2nd and 3rd reflectors. As a consequence, the total accumulated phase for both components after passing through the retro-reflector is the same. Since this compensation is independent of the reflection coefficients, the device is achromatic. The mirror version of this device is an attractive polarization rotator for ultra-short light pulses. The device in general can be used for broadband beams or for multi-line laser beams. CPS Beam displacers with $\Phi_{gp} = 0$ and π have also been reported [26].

An extension of the spin redirection phase is its manifestation in image-bearing optical beams. It is well known that the image in an image-bearing beam gets rotated when the beam is sent through a coiled fiber bundle, such as an endoscope, or through off-plane reflections [27]. Traditionally, image rotations via off-plane mirror reflections are calculated using matrix methods [28]. However, recognition that such a rotation is a manifestation of geometric phase has brought a new outlook to the problem [29]. Classic imaging systems can be understood from a simpler perspective [24]. For example, the Porro system with a variable angle between the two prisms, shown in Fig. 3, rotates images by the amount given by the geometric phase (see Fig. 3). The classic Porro image inverting system used in binoculars corresponds to the case $\alpha = \pi/2$, giving the image inverting condition $\Phi_{gp} = \pi$. Geometric phase also explains the image rotating properties of the Dove prism and the image inversion effected by a corner cube [24].

III. Pancharatnam Phase: transformations in the state of polarization

The geometric phase that arises from transformations in the state of polarization was first discovered by S. Pancharatnam in 1955 [30]. This phase was later interpreted as a manifestation of Berry's phase [31,32]. A comprehensive review of the fundamentals of this phase can be found in Ref. [32]. Unitary (intensity-preserving) transformations of the state of polarization can be described in the framework of Jones Vector algebra [33], which obeys SU(2) symmetry. All of the analysis used to obtain Pancharatnam phase can be done via the Jones vector algebra. However, the great power of geometric phase is its geometric, and thus visual character. At least at the design level, the geometric analysis appears much quicker and clearer than the matrix computation method. A graphical representation of the space of states of polarization is the Poincare sphere. This is a unit sphere where each state of polarization is represented by a point on its surface (see Fig. 5): the north and south poles represent the states right and left circularly polarizations |RCP> and |LCP>, respectively. Points along the equator represent linear polarization states of varying azimuth, with antipodes being orthogonal states. Other points $|\theta,\phi\rangle$ correspond to states of elliptical polarization given by

$$|\theta,\phi\rangle = \cos(\theta/2)\ \exp(-i\phi/2)\ |RCP\rangle + \sin(\theta/2)\ \exp(+i\phi/2)\ |LCP\rangle. \qquad (3)$$

In the Jones vector notation they are represented by

$$\begin{pmatrix} \cos(q/2)\exp(-if/2) \\ \sin(q/2)\exp(+if/2) \end{pmatrix}. \qquad (4)$$

The standard convention for transformations on the Poincare sphere are paths on the surface of the sphere that correspond to rotations about an axis that passes through the center of the sphere. The action of a wave plate is represented by a rotation about an axis

that passes through a point along the equator and the center of the sphere [34]. For example, suppose that we have a linearly polarized wave oriented along the *x*-axis (horizontally polarized). This is represented by point *A* in Fig. 5. Consider that the wave is incident on a retarder with phase retardation Δ and the fast axis oriented an angle φ with respect to the *x*-axis. The final state of polarization is obtained geometrically on the Poincare sphere via a rotation by an angle Δ about the axis *OR*, which forms an angle of 2φ with the *x*-axis. Thus the final state is described by point *B* in Fig. 5. If $\Delta = \pi/2$ (quarter-wave plate) and $\varphi = \pi/4$, then the path will be a quarter circle that connects *A* with *C*, with the latter representing the right circularly polarized state.

For a path that encloses an area Ω, the geometric phase is given by [31]

$$\Phi_{gp} = -\Omega/2. \tag{5}$$

Since it is purely geometrical in origin, as opposed to dynamical, it is inherently unbounded. That is, it can be increased indefinitely. Conversely, it is not absolute. That is, it has no memory of a previous phase, like the dynamical phase has, for example, via a displaced mirror. Nevertheless, this phase has many applications in polarization optics. This includes a variety of phase and frequency shifters and novel interferometers.

If the paths on the Poincare sphere involve only geodesic paths, then the phase is purely geometrical. Non-geodesic paths introduce dynamic phases arising from the birefringence of the optical medium [35]. A simple variable circular retarder is shown in Fig. 6a [35]. It consists of two half-wave plates with their fast axes forming an angle $\alpha/2+\pi/2$ relative to each other. If the input beam is right circularly polarized (RCP) and if the fast axis of the half-wave retarder forms an angle of $-\pi/4$ with the *x*-axis, which we label as $H(-\pi/4)$, then the state of polarization will follow the path *ABC* in Fig 6c. The second retarder with fast axis forming an angle $\alpha/2+\pi/4$ relative to the *x*-axis $[H(\alpha/2+\pi/4)]$ returns the beam to its original state via the path *CDA*. The solid angle enclosed by the path is 2α, and thus $\Phi_{gp} = \alpha$. If the angle of the second half-wave plate is increased by β then the return path will be *CEA*, and the area enclosed by the curve will increase by 4β, thus increasing Φ_{gp} by 2β.

A variable linear retarder for horizontal polarization can be constructed in a similar way (Fig. 6b): a quarter-wave plate $Q(-\pi/4)$ takes the state of polarization through path *BC*, $H(\alpha/2+\pi/4)$ continues with *CDA* and finally, $Q(-\pi/4)$ returns the light to the initial state via the path *AB*. Similarly to the circular retarder, increasing the angle of the half-wave retarder to $H(\alpha/2+\pi/4+\beta)$ increases the magnitude of the geometric phase by 2β. Other devices that have been proposed include variable [35] and half-wave [36] retarders for any state of polarization, compensators [37], polarization transformers between any two states [38,39], and achromatic quarter-wave and half-wave transformers [40]. Some of these devices involve non-geodesic paths on the Poincare sphere. In such cases the total phase for a closed path is the sum of the geometric phase and the dynamic phase [41]. A simple prescription for obtaining the dynamic phase has been described in Ref. [35]. However, it has been pointed out recently that that a non-geodesic path produced by a wave plate can be decomposed into a pair of geodesics that connect the initial and final state via an eigenstate of the wave plate (i.e., fast axis) [42]. With such a construction one

can express any closed path produced by wave plates as one consisting of purely geodesics, with the total phase being then purely geometric.

Geometric-phase-shifting can be used to measure the drift of an input signal. The interference of the signal and a phase-shifted reference beam from a local oscillator can be adjusted for maximum sensitivity by rotating the retarder using the error output signal of a detector that measures the interference [37]. A recording of the rotation of the retarder will be a measure of the phase drift of the signal. The advantage of this method is the endless phase control provided by geometric phase.

There are a number of interferometers working with the same group of phase shifters. Two interesting examples are shown in Fig. 7. The one in Fig. 7a is a Michelson interferometer with two quarter-wave plates on one of its arms [43, 44]. After the linearly polarized input (say parallel to the plane containing the beams) passes through the first retarder (with fast axis at $\pi/4$ relative to the polarization of the beam) it becomes circularly polarized. The second quarter-wave plate forming an angle $\alpha/2$ with the incident polarization puts the beam in a state of linear polarization. This wave plate is traversed twice by the action of the mirror, effectively acting as a half-wave plate. The second pass through the first wave plate returns the beam to the original state. Thus, the complete path is identical to the path *BCDAB* in Fig. 6c. A constant accumulation of phase results in a frequency shift. A few of these interferometers have been used as phase shifters before the concept of geometric phase was known [45].

The Sagnac interferometer of the type shown in Fig. 7b can be used for interferometry and phase shifting [46], even with white light [47]. The advantage of this system is that since both arms of the interferometer use the same path it is insensitive to variations in the optical path length and vibrations of the mirrors. In the interferometer shown, the horizontally (vertically) polarized beam traveling counter-clockwise (clockwise) acquires a geometric phase $+\alpha$ ($-\alpha$). The relative phase between the two counter-propagating beams when they recombine is 2α, and thus can be used as a stable phase shifter. An increase in the angle of the half-wave plate by β results in a relative phase increment of 4β. Operations with other states of polarization can be achieved by changing the type of retarder [48].

The interferometer shown schematically in Fig. 8a is used for nulling interferometry [49]. Briefly, two separate unpolarized but coherent beams are projected onto the same linearly polarized state *A*, shown in Fig. 8b. The polarizers following them project each beam onto orthogonal states *B* and *B´*. The two beams, superimposed with a polarizing beam splitter, pass through a variable linear retarder of the type described in Fig. 6b, each describing paths *BCEDB* and *B´DE´CB´*, which enclose geometric phases $-\alpha$ and $+\alpha$, respectively. The final states *B* and *B´* are then projected to state A via a polarizer. The phase difference between the two beams is 2α. The interesting aspect of this interferometer is that the phase shifts are accumulated *after* the beams have been recombined, a unique aspect of Pancharatnam phase. The accumulation of geometric phase after recombination also has applications in surface profiling [50]. Geometric phase

shifting can be used for direction control in antenna arrays, or for making a phase lens [51].

The geometric phase can be obtained from non-unitary paths. Normally these involve a projection using a polarizer, and thus a non-unitary transformation. Nevertheless, the geometric phase still appears. This method was used for the first demonstration of Pancharatnam phase [19]. One arm of the interferometer has two quarter-wave plates performing the paths *BA* and *AD* in Fig. 6c. The polarizer that follows projects state *D* onto state *B*, closing the circuit. The geometric phase is then $\Phi_{gp} = \alpha/2$. Another variation uses a half-wave plate as a second retarder [52], resulting in the path *BA*, *ADC*, and *CB* via the projecting polarizer.

Another type of device uses the geometric phase with unclosed paths on the Poincare sphere. The geometric phase is then obtained by "closing" the path with an imaginary geodesic. A retarder of this type may be one consisting of a quarter-wave plate converting the linear polarization to circular polarization and then projecting the latter state onto a linearly polarized state non-unitarily using a polarizer [53]. An interesting application of this involves interfering two coherent beams that are orthogonally polarized as shown in Fig. 9a. The corresponding states are represented by *B* and *B´* on the Poincare sphere. One beam can be a reference beam and the other could be the test beam (e.g., after passing through a non-uniform sample). The beams are sent through a quarter-wave plate with fast axis oriented $\pi/4$ relative to the two polarizations, which send the beams in separate paths on the Poincare sphere to the RCP and LCP states *C* and *D*, respectively, as shown in Fig. 9b. A polarizer oriented by an angle α relative to the *x*-axis projects the beams onto the state *E*. The phase for each beam is obtained by "closing" the paths with imaginary geodesics *EB* and *EB´*, giving geometric phases $\Phi_{gp} = \alpha$ and $\Phi'_{gp} = \pi/2 - \alpha$, respectively. Thus the phase difference between the two beams is $\Delta\Phi_{gp} = 2\alpha - \pi/2$. By changing α one can shift the fringes in the interference pattern [54]. The system can be used for locking onto a relative phase between the two beams [55]. This type of interferometer has been used as a vibration sensor in phase shifting interferometry [54,56], and in low-coherence interference microscopy [57].

A unique aspect of geometric phase is its non-linearity for certain paths on the Poincare sphere. If two points in a certain path are nearly antipodes of each other, a small change in one of them via a tuning element (e.g., wave plate, polarizer) may lead to large changes in the geodesic connecting the two points, and thus large changes in the geometric phase [58-60]. This may be used for supersensitive polarization interferometry [61], and optical switching [62,63]. Shown in Fig. 10a is a particularly simple and illustrative example of this non-linearity [63]. A beam of linearly polarized light is incident on a Michelson interferometer. The beam is polarized parallel to the *x*-axis, and split by a 50-50 beam splitter, which we will assume to be ideal. On each arm is a retarder with $\Delta << \pi/2$, but with fast axes oriented $\pm \pi/4$ relative to the *x* axis. When the beams are recombined they are in states *B* and *B¢*, as shown in Fig. 10b. A polarizer forming an angle θ with the *x*-axis projects these states onto state *C*. As θ is increased, the final state moves along the equator ($C \rightarrow C¢ \rightarrow C¢¢$ in Fig. 10b). One can see that as $\theta \rightarrow \pi/2$ the geodesics connecting *B* and *B¢* to *C* swing abruptly from lying close to the

equator to lying along a meridian. The value of Φ_{gp} (sum of the areas for the paths *ABC* and *A B′C* closed by the imaginary geodesic *CA*) increases from nearly zero for $\theta < \pi/2$, to $\Phi_{gp} = \pi$ for $\theta = \pi/2$, to $\Phi_{gp} \to 2\pi$ for $\theta \to \pi$. Figure 11 shows experimental data confirming the non-linearity [63]. One caveat about the use of the non-linearity of Pancharatnam phase: at the point of highest non-linearity ($\theta = \pi/2$ in this case) the interfering beams are nearly orthogonal, and thus the visibility of the fringes reduces to zero [63].

IV. Phase of transformations in the transverse modes of Gaussian beams

In recent years there has been much interest in paraxial optical beams carrying orbital angular momentum [64,65]. These are beams that contain a phase singularity or vortex in their transverse profile. They are represented by Laguerre-Gauss functions, which are solutions to the paraxial wave equation [66]. The field amplitude of a given mode can be expressed as [65]

$$LG_p^l(r,\phi,z) \propto r^l \exp[-r^2/w^2]\, L_p^l(2r^2/w^2) \exp[-ikr^2/(2R)] \exp(-il\phi) \exp[i(2p+l+1)\psi], \quad (6)$$

where w is the waist of the beam, R is the radius of curvature of the phase front, L_p^l is the associated Laguerre function, and ψ is the Gouy phase. These constitute a complete set of functions with cylindrical symmetry. Hermite-Gauss functions constitute a complete set of functions with rectangular symmetry.

$$HG_{nm}(x,y,z) \propto \exp[-(x^2+y^2)/w^2]\, H_n(2^{1/2}x/w)\, H_m(2^{1/2}y/w) \exp[-ik(x^2+y^2)/(2R)] \exp[-i(n+m+1)\psi], \quad (7)$$

where H_n is a Hermite function of order n. A variety of laser modes can be represented by either of these sets of functions. However, only recently were transformations between these modes developed and studied. These transformers use cylindrical lenses to alter the phase composition of beams via the Gouy phase [64].

A geometric phase for transformations between transverse modes was first proposed by van Enk [67]. A later experiment measuring the frequency shift of a rotating Laguerre-Gauss beam can be interpreted as a varying geometric phase [68]. Demonstrations of this phase for transformations of first-order modes have come only recently, in the mm-wave regime [69] and in the visible [70]. First-order modes can be represented by combinations of either two HG eigenstates or two LG eigenstates. As such, one can define a Poincare sphere for first-order modes [71,72], as shown in Fig. 12b. Similarly to the Poincare sphere for polarization states, the poles of the sphere are the LG modes of opposite helicity and the points along the equator represent HG modes of different azimuth. Pairs of cylindrical lenses can be used to make "$\pi/2$" and "π" converters [64,73]. A $\pi/2$ mode converter can convert a LG_0^1 mode into a HG_{10} mode and vice versa. Similarly, a π mode converter can convert a LG_0^1 mode to a LG_0^{-1} mode and vice versa. The $\pi/2$ and π mode converters are analogous to the quarter-wave and half-wave plates for polarization. Suppose we have two π mode converters in series, oriented an angle α relative to each other like in Fig. 12a. A beam in a LG_0^1 mode passing through them will make the light beam follow a closed path in mode space (solid lines in Fig. 12b), accumulating a geometric phase $\Phi_{gp} = 2\alpha$. Conversely, a beam in a LG_0^{-1} mode will follow a similar path

of opposite sense (dashed lines in Fig. 12b), acquiring a geometric phase $\Phi_{gp} = -2\alpha$. Since a HG_{10} mode tilted an angle θ relative to the x-axis can be expressed as

$$HG_{10}(x',y') = 2^{1/2} LG_0^1(r,\phi)\exp(i\theta) + 2^{1/2} LG_0^{-1}(r,\phi)\exp(-i\theta), \quad (8)$$

where $x' = x\cos\theta + y\sin\theta$, $y' = y\cos\theta - x\sin\theta$, with $x = r\cos\phi$ and $y = r\sin\phi$, then a HG_{10} beam incident on the two consecutive π rotators forming an angle α relative to each other (Fig. 12a) will be rotated by angle 2α. This has been recently verified experimentally [70].

The interesting aspect of high-order gaussian beam modes is that at higher orders the mode space increases. The development of a general formalism for the phase in mode orders greater than one still needs to be developed, but applications are already visible. It should explain the use of π converters as image rotators. Mode rotations have been used for axial control of biological samples in optical tweezers [74,75]. Geometric phases for modes LG_0^l should scale with l [68,76], thus increasing the capabilities of geometric-phase-based frequency shifters. More fundamentally, higher-order modes have the potential for being major players in quantum computation [77], where the use of geometric phase has recently been proposed [78].

V. Other Phases

As far as these optical phases have been investigated, they are independent of each other. More specifically, spin redirection and Pancharatnam phases have been shown to be additive when introduced independently [79]. However, when introduced in conjunction they need special treatment [80-82]. An application of this in interferometric imaging of microstructures has recently been proposed [83].

Spin redirection phase can be understood in terms of the SO(3) group of rotations in real space, while Pancharatnam phase and the phase of transformations of first-order modes is described by the SU(2) group of transformations [32,72]. All of the above can be represented graphically and easily on the surface of a sphere. The group-theoretical framework for transformations of higher-than-one modes of gaussian beams has yet to be developed, but it is anticipated that it will involve a higher-dimensional group of transformations and perhaps a not-so-easy-to-visualize multidimensional sphere. Other Phases that have been proposed include squeezed states of light [84-86], which are represented by the SO(2,1) group of Lorentz transformations, or equivalently, paths on a unit hyperboloid. However, this new phase has yet to be investigated experimentally.

In summary, as illustrated in this article, geometric phase has found a fertile ground for applications in optics. Its unique characteristics make this phase a solid alternative to dynamical phases. Coming as a bonus is a form of analysis that relies on geometrical constructions, which makes it a simple framework for the design of new devices and applications. Since geometric phase depends on trajectories in parameter or state space, we only need to find new dynamical settings to encounter new manifestations of geometric phase and find new applications in optics. We can safely conclude that geometric phase is indeed boundless.

VI. Acnowledgements

The author thanks past and present collaborators M.W. Cheyne, P.J. Haglin, C.D. Holmes, P.M. Koch, J. Stewart, H.I. Sztul, and R. Williams for fruitful discussions, and funding from Research Corporation and NSF grant 9988004, and the Schlichting fund of Colgate University. The author also thanks Prof. Qu Li for kind permission to use his data for Fig. 11.

VII. References

[1] Berry, M.V., 1984, Proc. R. Soc. Lond. A, 392, 45.
[2] Anandan, J., Christian, j., and Wanelik, K., 1997, Am. J. Phys., 65, 180.
[3] Shapere, A., Wilczek, F., 1989, Geometric Phases in Physics, World Scientific, Singapore.
[4] Hannay, J.H., 1985, J. Phys. A, 18, 221.
[5] Tiwari, S.C., 1992, J. Mod. Opt., 39,1097.
[6] Rytov, S.M., 1938, Dokl. Acad., Nauk SSSR, 18, 263; english translation, 1989, Markovski, B., and Vinitsky, V.I., Topological Phases in Quantum Theory, World Scientific, Singapore, 6.
[7] Vladimirskii, V.V., 1941, Dokl. Acad., Nauk SSSR, 31, 222; english translation, 1989, Markovski, B., and Vinitsky, V.I., Topological Phases in Quantum Theory, World Scientific, Singapore, 11.
[8] Chiao, R., Wu, Y.-S., 1986, Phys. Rev. Lett., 57, 933.
[9] Haldane, F.D.M., 1986, Opt. Lett., 11, 730.
[10] Ryder, L.H., 1991, Europhys. Lett., 12, 15.
[11] Tomita, A., Chiao, R.Y., 1986, Phys. Rev. Lett., 57, 937.
[12] Ross, J.N., 1984, Opt. Quantum Electron., 16, 455.
[13] Wassmann, F., and Ankiewicz, A., 1998, Appl. Opt. 37, 3902.
[14] Frins, E.M., and Dultz, W., 1997, Optics Commun., 136, 354.
[15] Senthilkumaran, P., Thursby, G., and Culshaw, B., 2000, Opt. Lett., 25, 533.
[16] Zel'dovich, B. Ya., and Liberman, V.S., 1990, Sov. J. Quantum Electron., 20, 427.
[17] Zel'dovich, B. Ya., and Kundikova, N.D., 1995, Quantum Electron., 25, 172.
[18] Volyar, A.V., Zhilaitis, V.Z., Fadeeva, T.A., and Shvedov, V.G., 1998, Tech. Phys. Lett., 24, 322.
[19] Bhandari, R., and Samuel, J., 1988, Phys. Rev. Lett., 60, 1211.
[20] Kwon, O.J., Lee, H.T., Lee, S.B., and Choi, S.S., 1991, Opt. Lett., 16, 223.
[21] Chiao, R., Antaramian, A., Ganga, K.M., Jiao, H., Wilkinson, and S.R., Nathel, H., 1988, Phys. Rev. Lett., 60, 1214.
[22] Kitano, M., Yabuzaki, and T., Ogawa, T., Phys. Rev. Lett., 58, 523.
[23] Galvez, E.J., and Koch, P.M., 1997, J. Opt. Soc. Am., 14, 3410.
[24] Galvez, E.J., and Holmes, C.D., 1999, J. Opt. Soc. Am. A, 16, 1981.
[25] Galvez, E.J., Cheyne, M.R., Stewart, J.B., Holmes, C.D., and Sztul, H.I., 1999, Optics Comm., 171, 7.

[26] Galvez, E.J., 2001, Opt. Lett., 26, 971.
[27] Swift, D.W., 1972, Opt. Laser Technol., Augiust, 175.
[28] Hopkins R.E., 1965, Appl. Opt. Opt. (CHECK) Eng. 3, 269.
[29] Segev, M., Solomon, R., and Yariv, A., 1992, Phys. Rev. Lett., 69, 590.
[30] Pancharatnam, S., 1956, Proc. Indian Acad. Sci. Sect. A, 44, 247; reprinted in 1975, Collected Works of S. Pancharatnam, Oxford Univ. Press, London.
[31] Berry, M.V., 1987, J. Mod. Opt., 34, 1401.
[32] Bhandari, R., 1997, Phys. Rep., 281, 1.
[33] Azzam, R.M.A., and Bashara, N.M., 1989, Ellipsometry and Polarized Light, North Holland, Amsterdam.
[34] Jerrard, H.G., 1954, J. Opt. Soc. Am, 44, 634.
[35] Bhandari, R., 1989, Phys. Lett. A, 138, 469.
[36] Bhandari, R., 1997, Appl. Opt., 36, 2799.
[37] Martinelli, M., and Vavassori, P., 1990, Optics Comm., 80, 166.
[38] Simon, R., and Mukunda, N., 1989, Phys. Lett. A, 138, 474.
[39] Simon, R., and Mukunda, N., 1990, Phys. Lett. A, 143, 165.
[40] Hariharan, P., Ciddor, P.E., 1994, Optics Comm., 110, 13.
[41] Jordan, T., J. 1988, Math. Phys., 29, 2042.
[42] Courtial, J., 1999, Optics Comm., 171, 179.
[43] Simon, R., Kimble, H.J., and Sudarshan, E.C.G., 1988, Phys. Rev. Lett., 61, 19.
[44] Chyba, T.H., Wang, L.J., Mandel, L., Simon, R., 1988, Opt. Lett., 13, 1988.
[45] Bhandari, and R., Dasgupta, T., 1990, Phys. Lett. A, 143, 170.
[46] Hariharan, P., and Roy, M., 1992, J. Mod. Opt., 39, 1811.
[47] Hariharan, P., Larking, K.G., Roy, M., 1994, J. Mod. Opt., 41, 663.
[48] Hariharan, P., 1993, J. Mod. Opt., 40, 985.
[49] Baba, N., Murakami, N., and Ishigaki, T., Opt. Lett., 2001, 26, 1167.
[50] Hariharan, P., Roy, M., 1994, J. Mod. Opt., 41, 2197.
[51] Bhandari, R., 1995, Phys. Lett. A, 204, 188.
[52] Bhandari, R., 1988, Phys. Lett. A, 133, 1988.
[53] Suja Helen, S., Kothiyal, M.P., Sirohi, R.S., 1998, Optics Comm., 154, 249.
[54] Ferrari, J.A., Frins, E.M., Perciante, D., and Dubra, A., 1999, Opt. Lett., 24, 1272.
[55] Wehner, M.U., Ulm, M.H., and Wegener, M., 1997, Opt. Lett., 22, 1455.
[56] Ferrari, J.A., Frins, E.M., and Dultz, 1997, J. Lightwave. Technol., 15, 968.
[57] Roy, M., Svahn, P., and Sheppard, C.J.R., 2001, Proc. SPIE, 4417, 529.
[58]Bhandari, R., 1991, Phys. Lett. A, 157, 221.
[59] Bhandari, R., 1993, Phys. Lett. A, 180, 21.
[60] Schmitzer, H., Klein, S., and Dultz, W., Phys. Rev. Lett., 71, 1530.
[61] Hils, B., Dultz, W., Martienssen, W., 1999, Phys. Rev. E, 60, 2322.
[62] Tewari, S.P., Ashoka, V.S., and Ramana, M.S., 1995, Optics Commun., 120, 235.
[63] Li, Q., Gong, L., Gao, Y., and Chen, Y., 1999, Optics Commun., 169, 17.
[64] Allen, L., Beijersbergen, M.W., Spreeuw, R.J.C., and Woerdman, J.P., 1992, Phys. Rev. A, 45, 8185.
[65] Allen, L., Padgett, M.J., and Babiker, M., 1999, Progress in Optics XXXIX, Elsevier, 291.
[66] Siegman, A., 1986, Lasers, University Science Books, Mill Valley.
[67] van Enk, S.J., 1993, Optics Commun., 102, 59.

[68] Courtial, J., Dholakia, K., Robertson, D.A., Allen, L., and Padgett, M.J., 1998, Phys. Rev. Lett., 80, 3217.
[69] Brandt, G.F., 2000, Int. J. Infrared Millimeter Waves, 21, 505.
[70] Galvez, E.J., and Sztul, H.I., (to be published in Coherence and Quantum Optics VIII).
[71] Padgett, M.J., and Courtial, J., 1999, Opt. Lett., 24, 430.
[72] Agarwal, G.S., 1999, J. Opt. Soc. Am., 16, 2914.
[73] Beijersbergen, M.W., Allen, L., van der Veen, H.E.L.O., and Woerdman, J.P., 1993, Optics Commun., 96, 123.
[74] Sato, S, Ishigure, M., and Inaba, H., 1991, Electron. Lett., 27, 1831.
[75] Sztul, H.I., Haglin, P.J., Weiss, A., and Galvez, E.J., 2001, Meeting of the Optical Society of America.
[76] Nienhuis, G., 1996, Optics Commun., 132, 8.
[77] Mair, A., Vaziri, A., Weihs, G., and Zeilinger, A., 2001, Nature, 412, 313.
[78] Duan, L.-M., Cirac, J.I., and Zoller, P., 2001, Science, 292, 1695.
[79] Jiao, H., Wilkinson, S.R., Chiao, R.Y., and Nathel, H., 1989, Phys. Rev. A, 39, 3475.
[80] Bhandari, R., 1991, Physica D, 175, 111.
[81] Hannay, J.H., 1998, J. Mod. Opt., 45, 1001.
[82] Tavrov, A.V., Miyamoto, Y., Kawabata, T., Takeda, M., and Andreev, V.A., 2000, J. Opt. Soc. Am. A, 17, 154.
[83] Tavrov, A.V., Miyamoto, Y., Kawabata, T., Takeda, M., and Andreev, V.A., 2000, Opt. Lett., 25, 460.
[84] Chiao, R.Y., Jordan, T.F., 1988, Phys. Lett. A, 132, 77.
[85] Gerry, Ch. C., 1989, Phys. Rev. A, 39, 3204.
[86] Leonhardt, U., 1993, Optics Commun., 104, 81.

List of Figures:

Figure 1. (a) Example of an optical fiber describing a coiled path. (b) Corresponding path *C* enclosing the area Ω described by the spin vector of the light on the sphere of directions.

Figure 2. (a) Example of a coiled optical path using discrete reflections. (b) Corresponding path of the spin vector $\mathbf{k}\updownarrow$ on the sphere of directions, formed by connecting consecutive spin vectors with geodesics.

Figure 3. (a) Diagram of the prism-based variable-angle Porro rotator. (b) Corresponding paths of the propagation direction (*S*) and spin (*C*) on the sphere of directions.

Figure 4. Diagram of a geometric phase rotator that is achromatic by compensating the reflection phases separately over two sets of orthogonal reflections.

Figure 5. Poincare sphere showing the paths described by the state of polarization of an input beam linearly polarized along the x-axis (OA) passing through: (a) a general Δ

retarder oriented by φ relative to OA (path AB), or (b) a quarter-wave plate oriented by π/4 relative to OA (path AC).

Figure 6. Schematic diagrams of (a) circular and (b) linear polarization retarders based on Pancharatmnam phase, and (c) the corresponding paths of the state of polarization on the Poincare sphere.

Figure 7. Schematic diagram of (a) Michelson-type and (b) Sagnac-type of Pancharatnam-phase-based interferometers.

Figure 8. (a) Schematic diagram of an interferometer based on non-unitary projections, with the Pancharatnam phases of the interfering beams accumulated after recombination. (b) Corresponding paths of the light beams on the Poincare sphere.

Figure 9. (a) Schematic of a Pancharatnam-phase-based interferometer for unclosed paths. (b) Corresponding Poincare sphere representation.

Figure 10. (a) Schematic of the setup to make a Pancharatnam-phase optical switch. (b) Paths of the state of polarization on the Poincare sphere as θ increases.

Figure 11. Experimental confirmation of the non-linearity of Pancharatnam phase for the setup of Fig. 10, where 2Δ for points *B* and *B*′ is 10° and 12°, respectively. The symbols are the data [63] and the solid line is the theoretical prediction.

Figure 12. (a) Schematic of a setup to rotate a HG10 mode: using two consecutive π mode converters with their axes forming an angle α relative to each other. (b) Light beams in initial modes LG_0^{1} and LG_0^{-1} passing through the two consecuting π mode converters respectively describe solid and dashed paths on the Poincare sphere of modes, and thus each acquiring respective geometric phases 2α and –2α.

Fig. 1

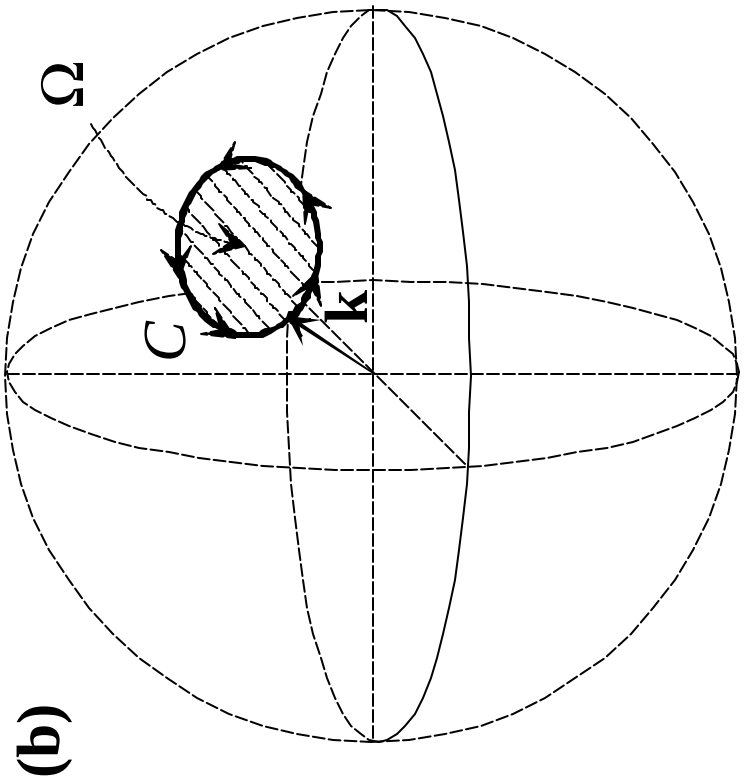

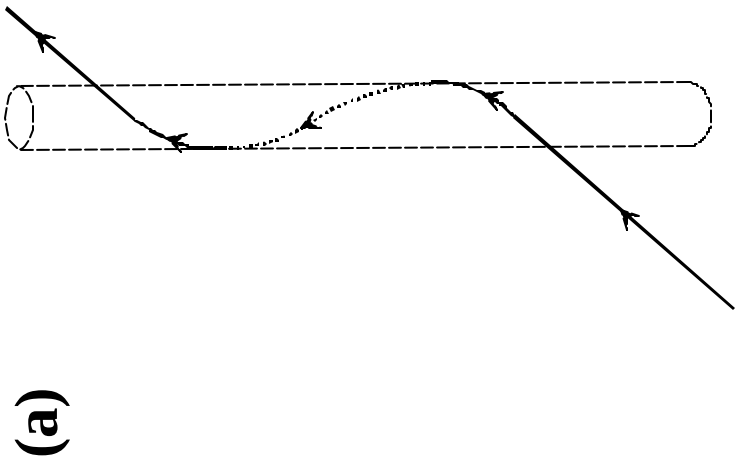

Fig. 2

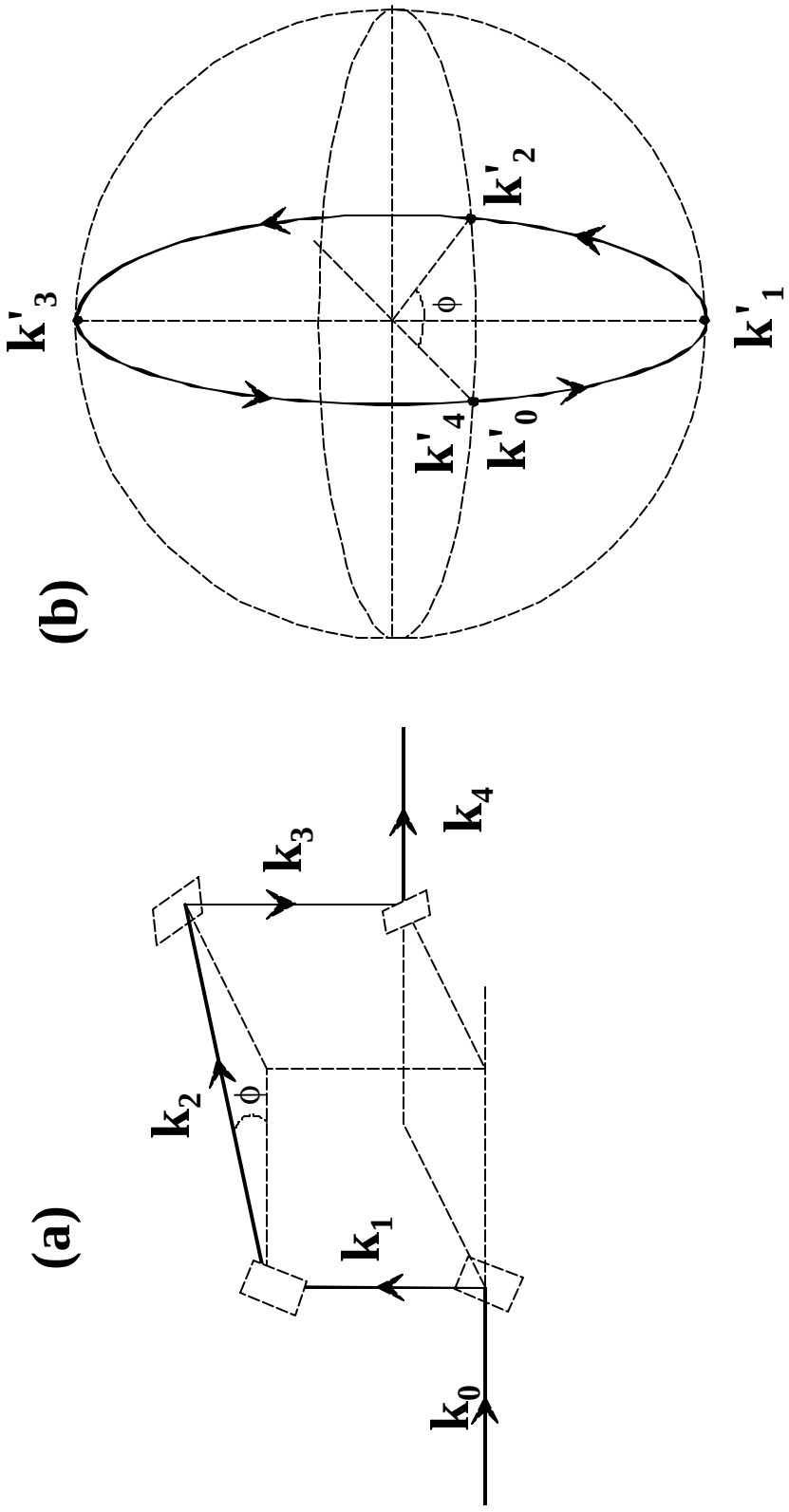

Fig. 3

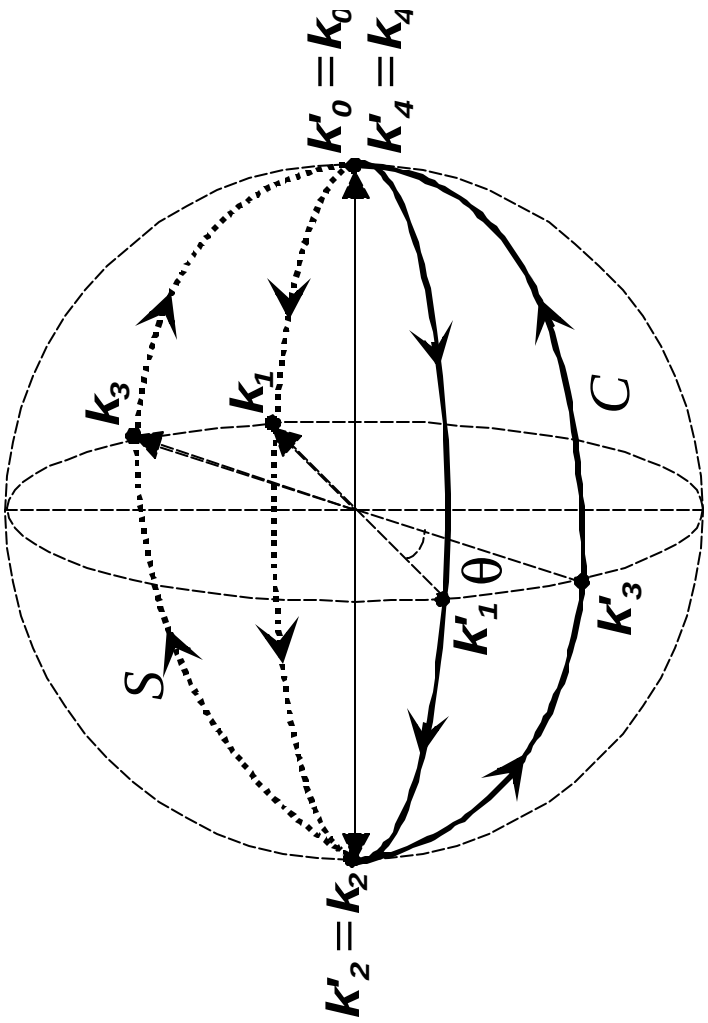

(b)

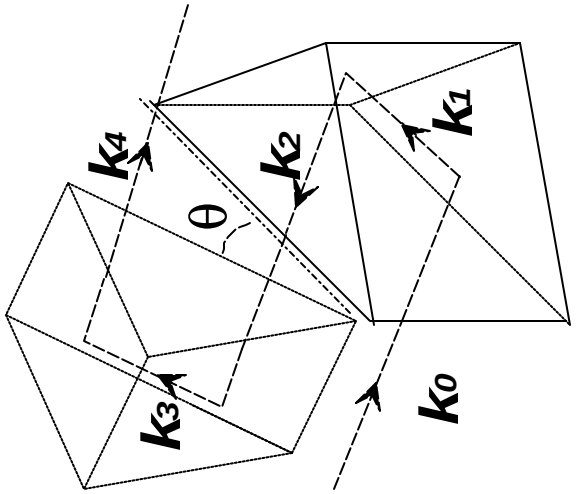

(a)

Fig. 4

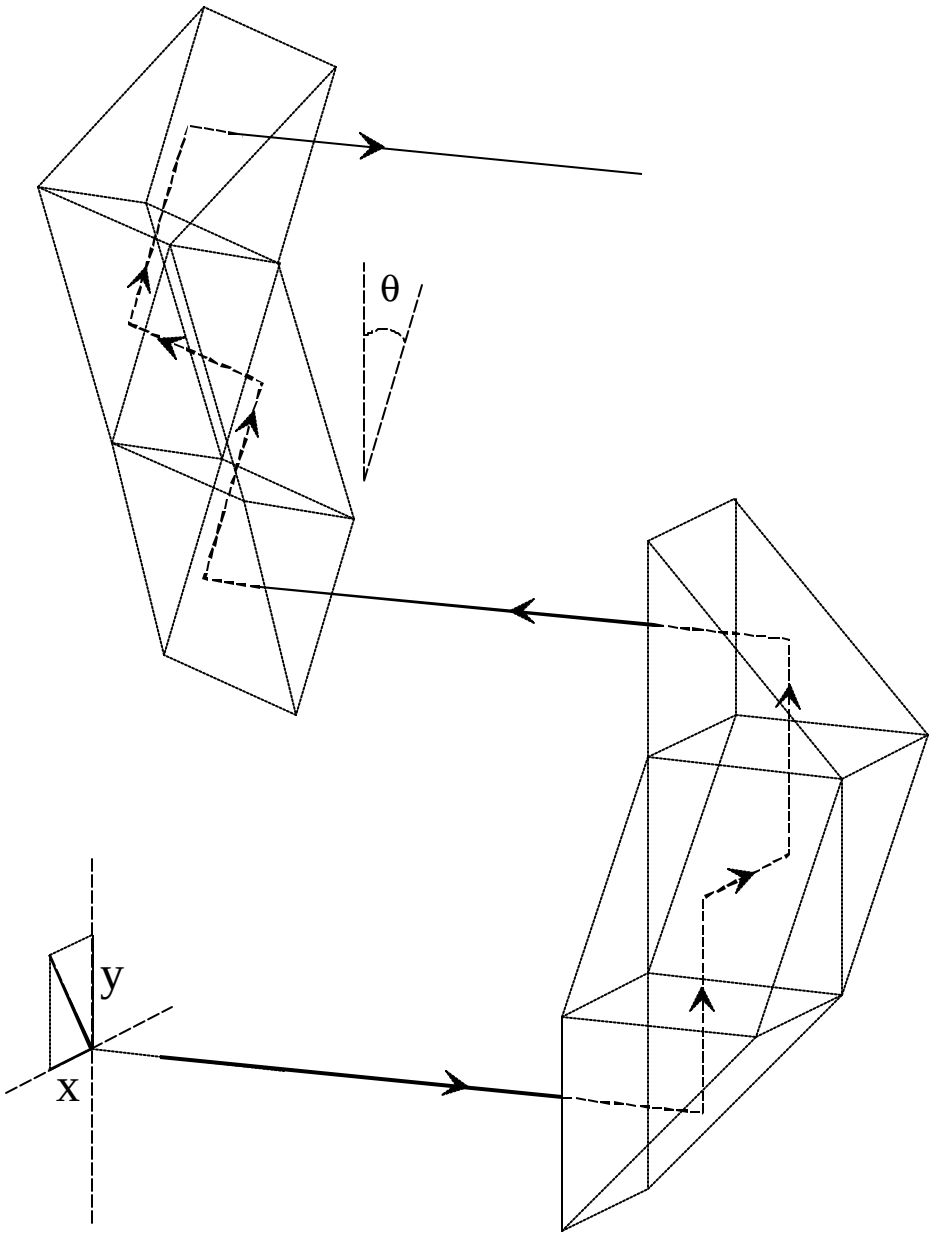

Fig. 5

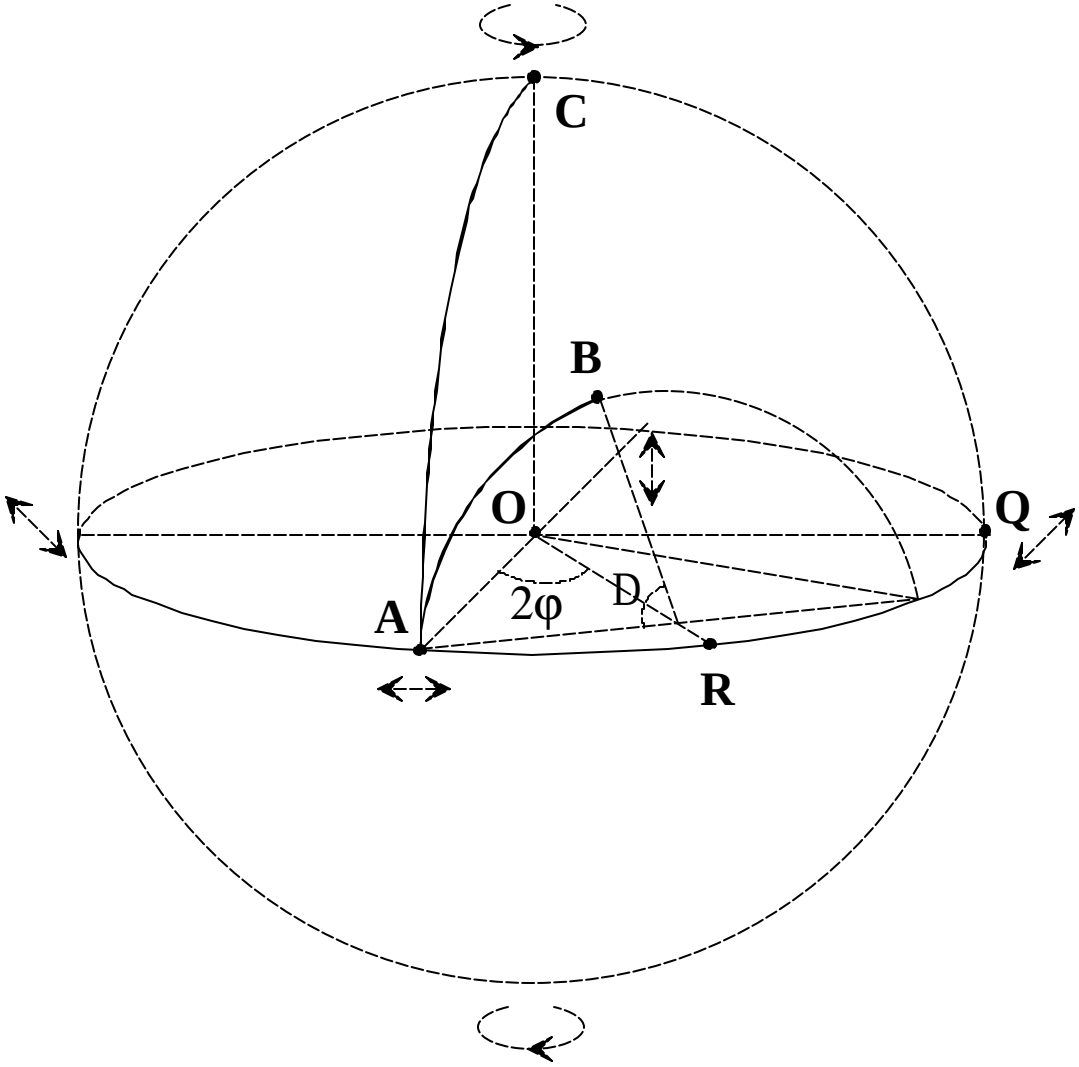

Fig. 6

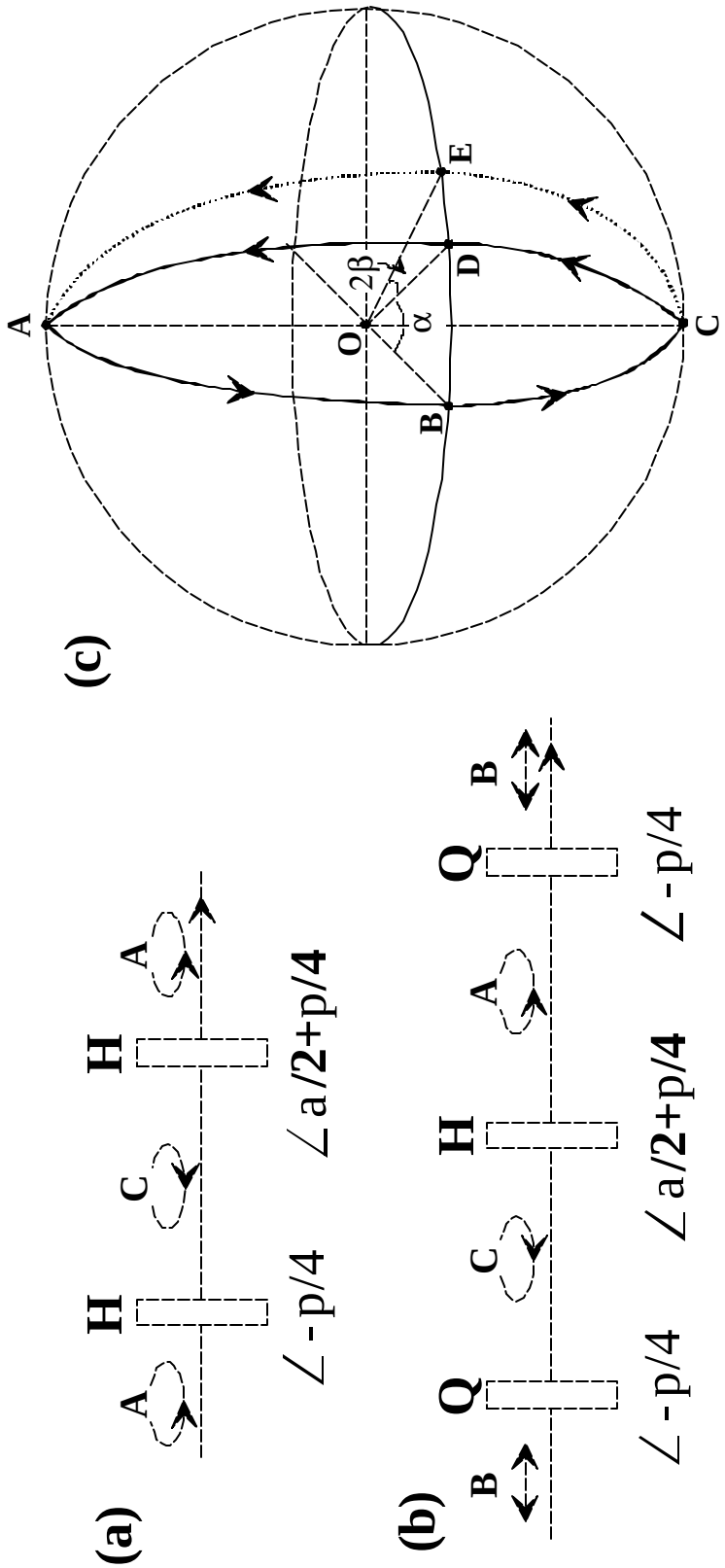

Fig. 7

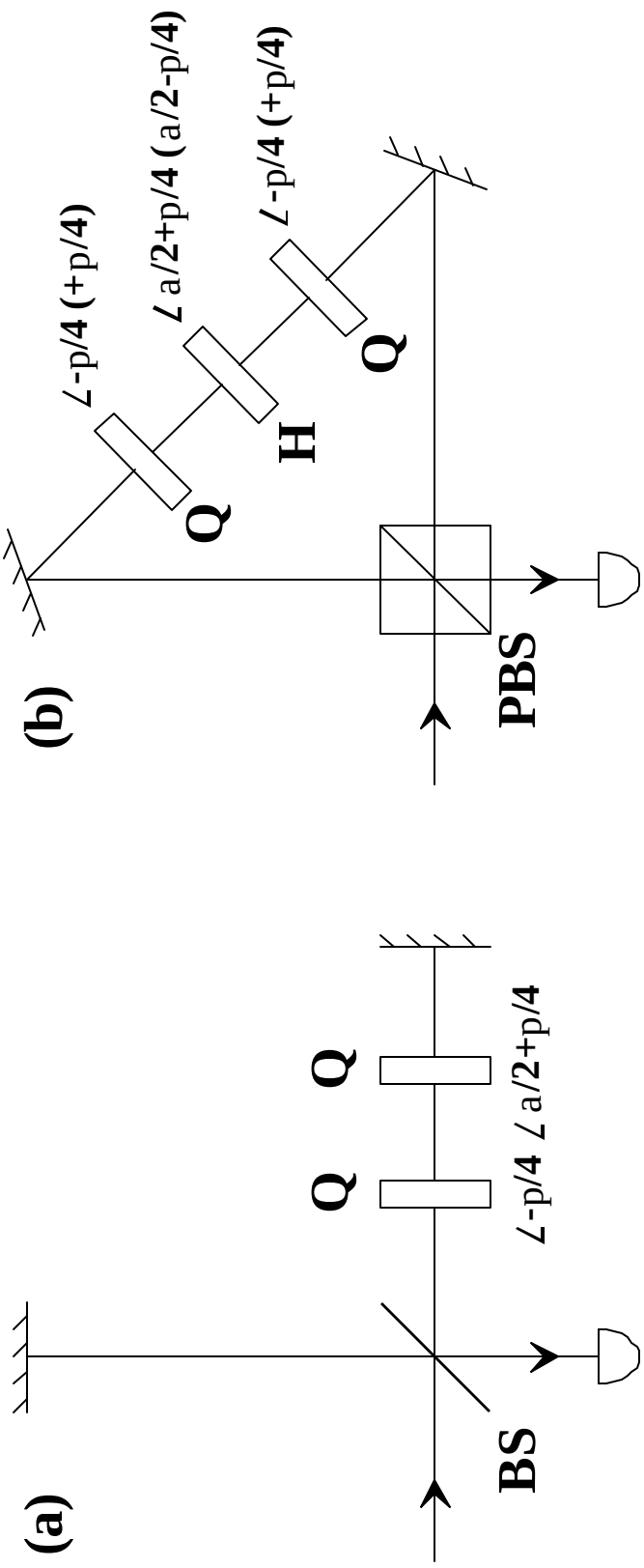

Fig. 8

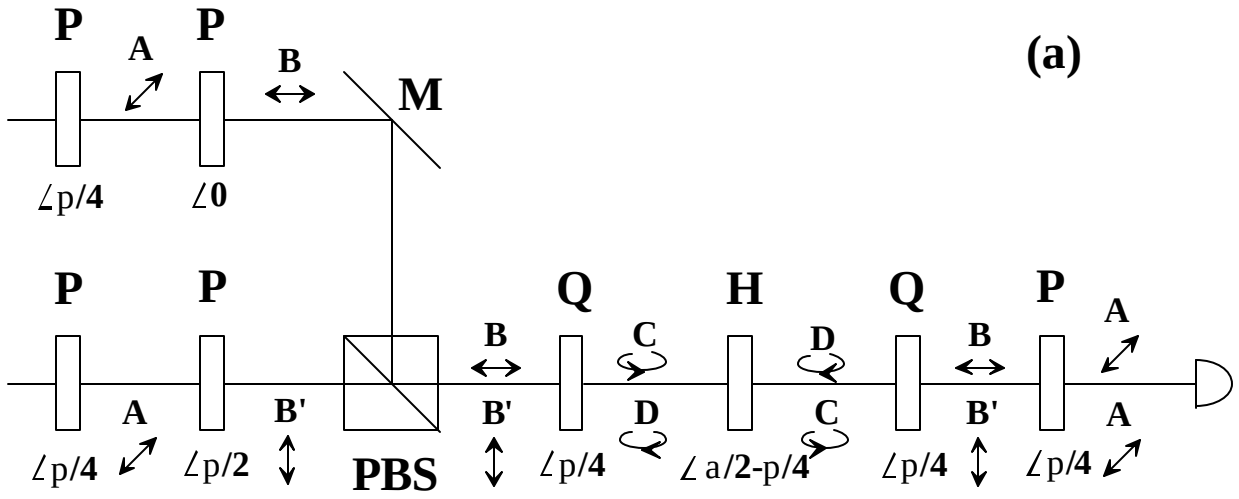
P
A
P
B
M
(a)
∠p/4
∠0
P
P
Q
H
Q
P
A
B
C
D
B
A
B'
B'
D
C
B'
A
∠p/4
∠p/2
PBS
∠p/4
∠a/2-p/4
∠p/4
∠p/4

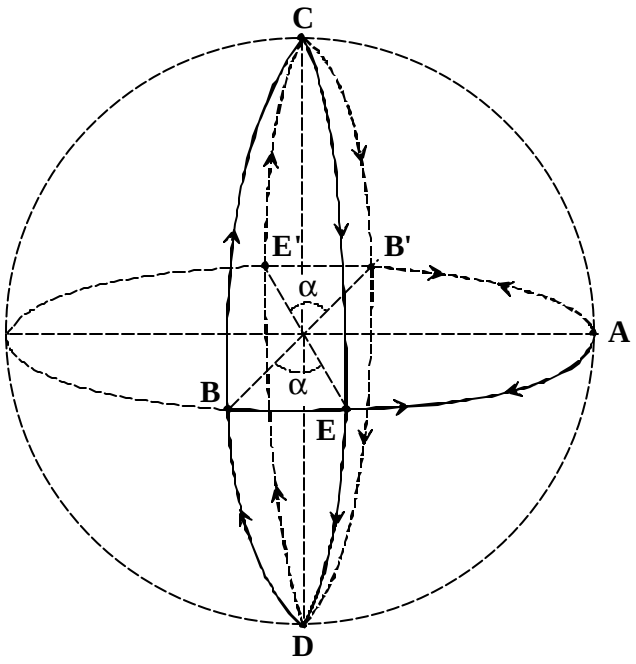
(b)
C
E'
B'
α
A
α
B
E
D

Fig. 9

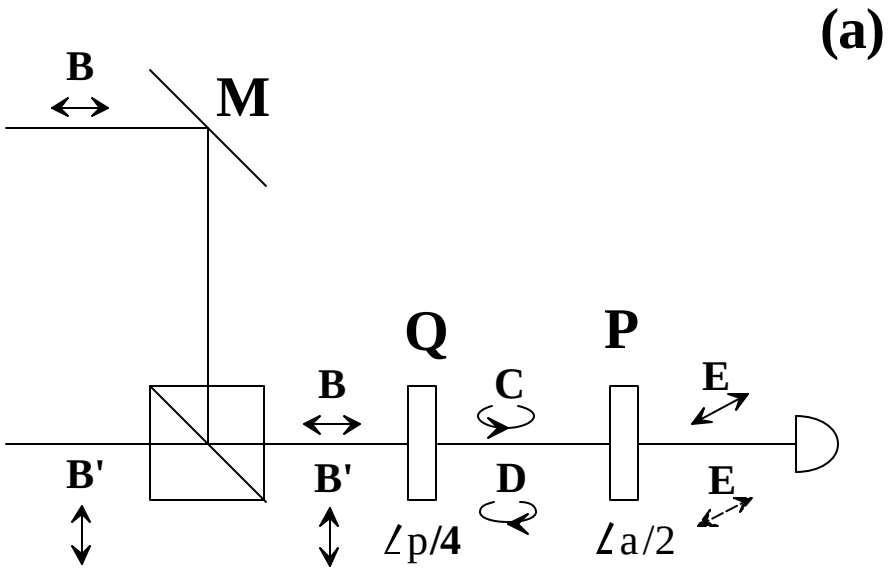

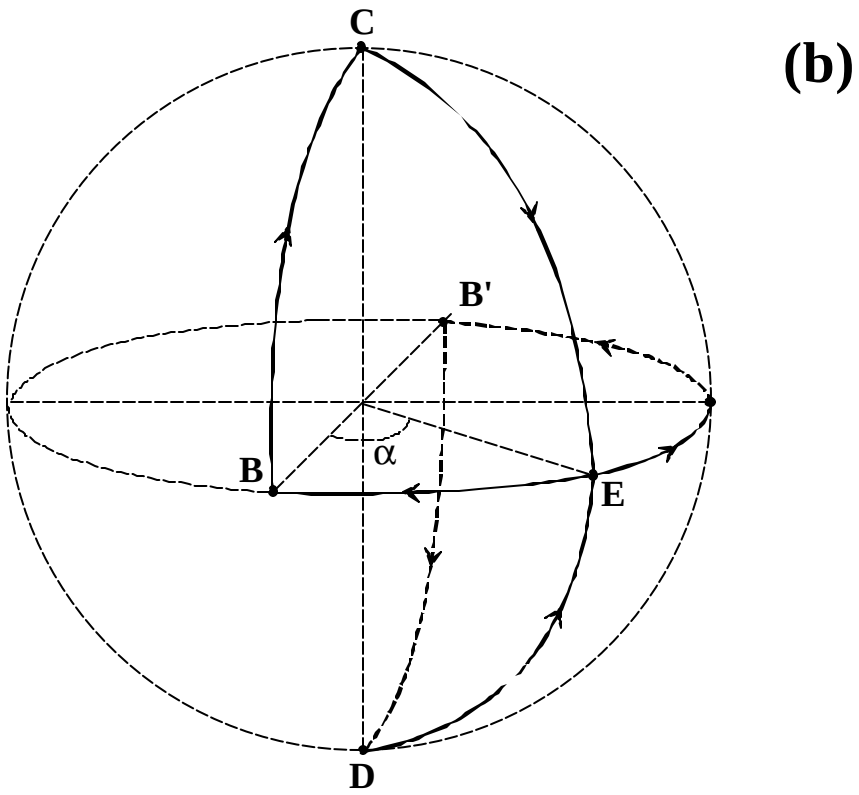

Fig. 10

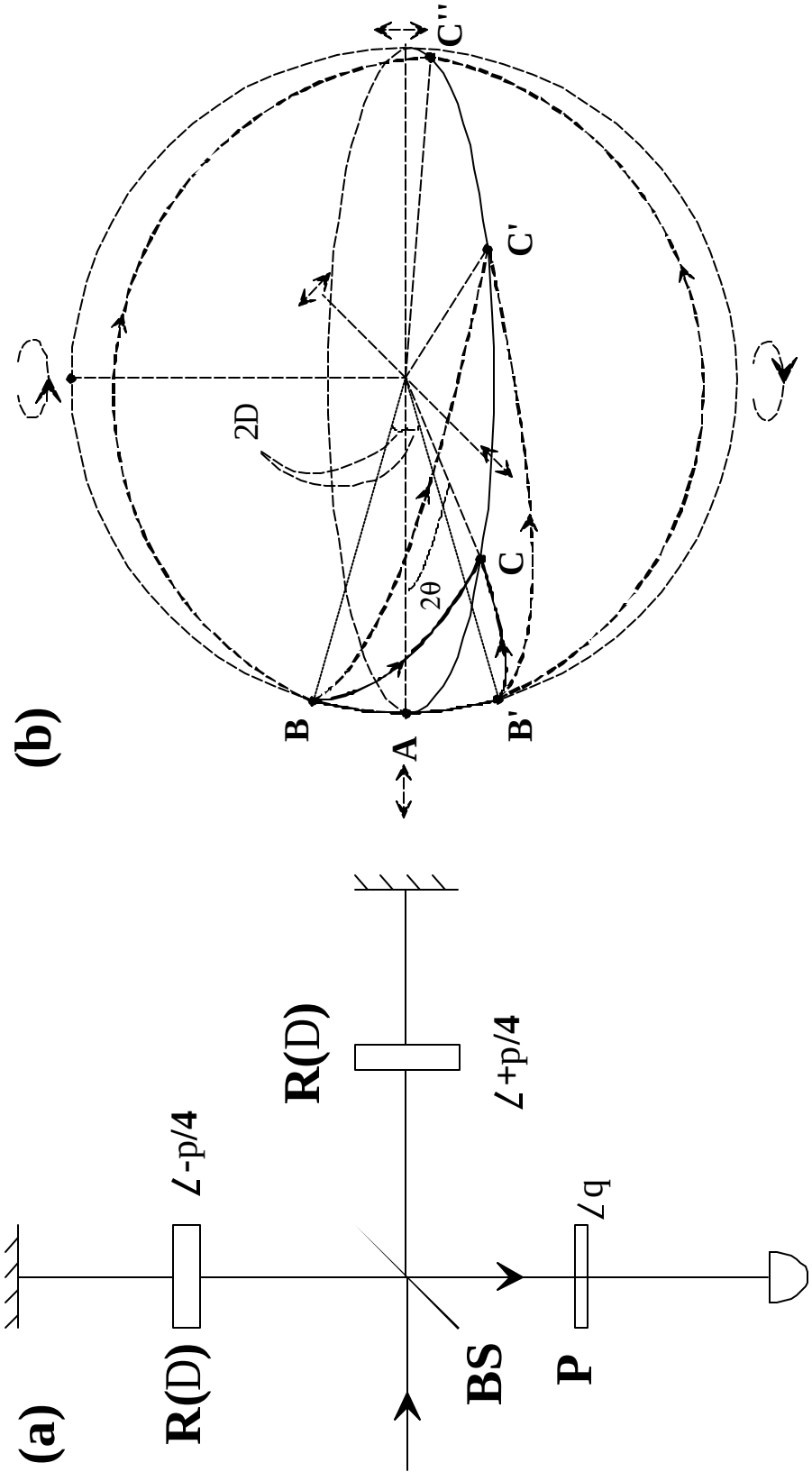

Fig. 11

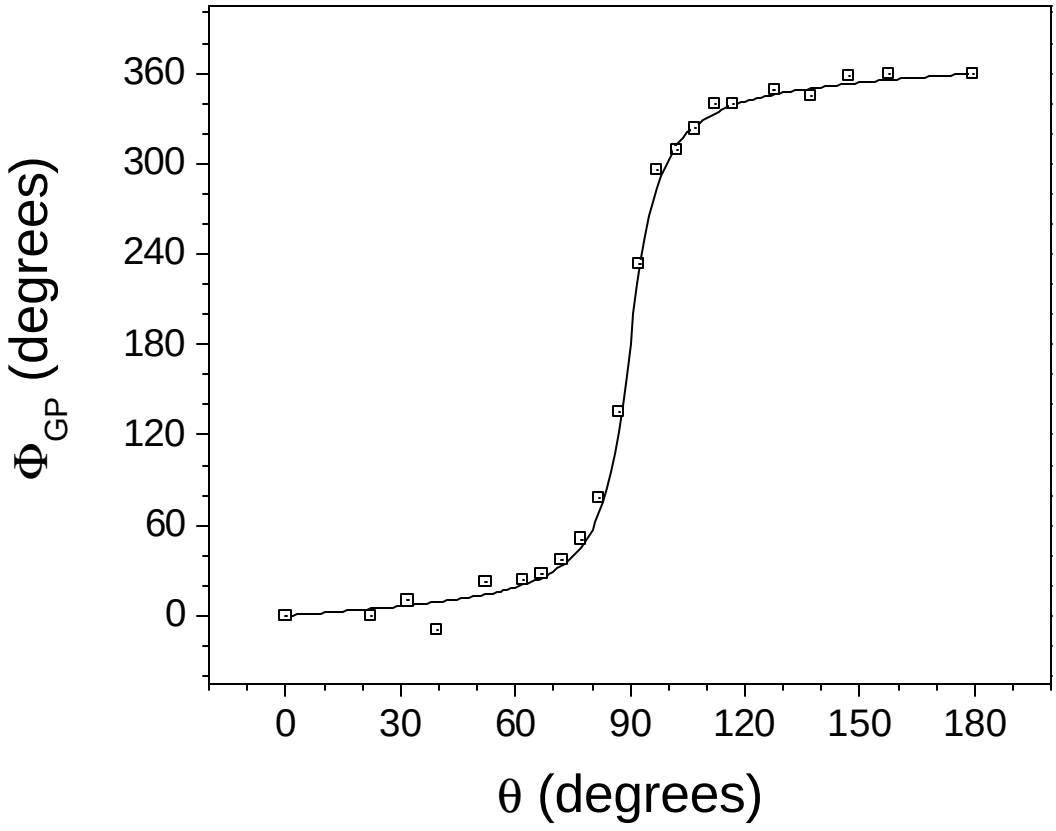
360
300
240
180
120
60
0
Φ_{GP} (degrees)
0
30
60
90
120
150
180
θ (degrees)

Fig. 12